Contents lists available at SciOpen

Food Science and Human Wellness

journal homepage: https://www.sciopen.com/journal/2097-0765

China Food Publishing Co.

Effects of black highland barley starch on regulating sustained glucose release and fluctuations in individuals with type 2 diabetes

Shuxin Deng[a,1], Xiaoguo Ji[a,b,1], Jiaming Wang[c], Liqiang Fan[a,b], Jiayang Jin[a,b,*], Juan Li[c,*], Liming Zhao[a,c,d,*]

[a]State Key Laboratory of Bioreactor Engineering, School of Biotechnology, East China University of Science and Technology, Shanghai 200237, China
[b]Shanghai Frontiers Science Center of Optogenetic Techniques for Cell Metabolism, Shanghai 200237, China
[c]Shanghai Changzheng Hospital, Shanghai 200003, China
[d]Shanghai Collaborative Innovation Center for Biomanufacturing Technology (SCICBT), Shanghai 200237, China

ARTICLE INFO

Article history:
Received 29 March 2024
Received in revised form 13 July 2024
Accepted 2 September 2024

Keywords:
Black highland barley
Starch structure
Type 2 diabetes
Glucose regulation
Gut metabolites

ABSTRACT

Consuming low-glycemic index foods, such as black highland barley (BHB), is essential for regulating post-meal glucose levels in individuals with type 2 diabetes mellitus (T2DM). This study examined how the starch structure of BHB affected glucose fluctuations. The incorporation of BHB enlarged starch granule size and modified the crystalline structure to an A + V type with a relative crystallinity of 31.14%. This alteration facilitated a more organized release of glucose. Population-based trials lasting 6 weeks had demonstrated that that BHB could reduce glucose variation, ghrelin levels, and insulin resistance in T2DM. Additionally, it increased the populations of beneficial gut bacteria such as *Akkermansia*, *Bifidobacterium*, and *Lactobacillus*, while also raising levels of gastric inhibitory peptides, phenolics, and specific gut metabolites. The specific digestion protocol and mathematical model of BHB disclosed its slow gastric emptying and glucose release rates, which were crucial for maintaining stable glucose levels in individuals with T2DM. Understanding the starch structure of BHB provided an effective dietary intervention for managing T2DM-related glucose fluctuations.

1. Introduction

Type 2 diabetes mellitus (T2DM) is a metabolic disorder characterized by chronic hyperglycemia resulting from an imbalance in glucose homeostasis, primarily due to insufficient insulin secretion or insulin resistance. In 2021, the global prevalence of diabetes in the 20−79 age group is 10.5%, and it is projected to rise to 11.3% by 2030 and 12.2% by 2045. Epidemiology shows that the prevalence of T2DM will reach 9.7% during the period 2020−2030[1]. The development of T2DM is mainly attributed to genetic and environmental factors such as obesity, lack of physical activity, and improper diet. Currently, injecting insulin is an effective way to control blood glucose. However, long-term use of insulin and oral medications can lead to drug dependence, drug resistance, weight gain, and hypoglycemia. The etiology of T2DM is largely believed to be associated with a diet that is high in nutrients and low in energy expenditure[2]. Therefore, dietary intervention is a crucial component of adjunctive therapy for T2DM.

Dietary interventions primarily focus on developing low glycemic index (GI) foods and analyzing related mechanisms that regulate blood glucose homeostasis. A meta-analysis demonstrates the relationship between carbohydrate quality indicators, such as dietary fiber, whole grains, GI, and glycemic load (GL), and the incidence and mortality rates of diseases like diabetes and cardiovascular disease. The quality, rather than the quantity, of carbohydrates has the most significant impact on health. Consumption of low GI/GL staple foods is shown to attenuate postprandial blood glucose fluctuations and

[1] These authors contributed equally to this work.
[*] Corresponding authors.
E-mail address: zhaoliming@ecust.edu.cn (L.M. Zhao); jinjiayang@ecust.edu.cn (J.Y. Jin); yyk3020@163.com (J. Li)
Peer review under responsibility of Beijing Academy of Food Sciences.

SciOpen Publishing services by Tsinghua University Press

http://doi.org/10.26599/FSHW.2024.9250390

maintain blood glucose stability[3]. Mixed grain products, represented by black highland barley (BHB), are considered indigestible and low GI foods.

BHB has higher nutritional value compared to traditional grains. Numerous studies have shown that BHB can effectively lower glucose, cholesterol, and lipoproteins, and has preventive and regulatory effects on various diseases in the human body[4-6]. Lu et al.[5] found that among boiling, extrusion, and milling treatments of BHB, extrusion resulted in less cell structure damage, lower digestion rate, and higher production of short-chain fatty acids after colonic fermentation. Consumption of BHB improved postprandial glucose and insulin response and led to normalization of amino acid and biogenic amine status[7]. Currently, there has been limited exploration of the structural aspects of BHB starch in a food matrix. The relationship between starch structure and digestibility remains unclear. In previous dietary interventions with BHB, the substitution rate of BHB was relatively low (around 20%−30%), and the mechanistic basis for the blood glucose-regulating function of BHB is not clearly explained.

The objective of this study was to clarify the mechanisms underlying the blood glucose-regulating effects of BHB starch. It was hypothesized that noodles containing BHB had a starch structure that regulated glucose release, thereby reducing postprandial glucose fluctuations, and improving blood glucose stability. The study elucidated the microstructure and crystal structure of BHB starch and then incorporated it into noodles with the potential to modulate glucose release. In a randomized crossover trial, blood glucose monitoring technology was used to assess the blood glucose-regulating capacity of BHB noodles (BHBN). The kinetics of starch digestion were elucidated, and the controlled release of glucose by BHB was demonstrated through *in vitro* simulated digestion and mathematical modeling. This study aimed to establish a theoretical foundation for the development and application of BHB.

2. Materials and methods

2.1 Materials

BHB (*Hordeum vulgare* subsp. *spontaneum*) powder was produced from Qinghai, China. The wheat and buckwheat powder were purchased from a local supermarket (Shanghai, China). *α*-Amylase (50 U/mg), gastric protease (250 U/mg), pancreatin (4× USP), and lipase (90 U/mg) were purchased from Sigma (Karlsruhe, Germany). AceQ® qPCR SYBR® green master mix, Fast pure plant total RNA isolation kit, HiScript II 1st strand cDNA synthesis kit, and SYBR were purchased from Vazyme (Nanjing, China).

2.2 Standard preparation of BHBN

The 30% BHBN (BHBN1) and 70% BHBN (BHBN2) were prepared in the laboratory[8]. The dough was prepared by thoroughly mixing a specific proportion of BHB flour and wheat flour, and adding a specific proportion of water and flour for about 10 min. The dough was then rolled 6−8 times using a noodle press, and the resulting pieces were placed in a fresh-keeping bag and sealed for 30 min to allow the dough to fully absorb water. Finally, the noodle machine rolled the dough into 0.8 mm strips and cut them into 2.0 mm wide strips. The noodles were dried until the moisture content reached 12%, then stored for later use. Wheat noodles (WN, 100% wheat powder (WP)) and coarse grain noodles (CN, 10% barley powder + 10% buckwheat powder + 80% WP) were prepared according to the method described above. The compositions (protein, fat, total starch, amylose, and dietary fiber) of the different proportions of BHB used in this study were listed in Table S1.

2.3 Microstructure and crystalline characterization of BHB starch

2.3.1 Observation of morphological characteristics of starch in BHB

The surface morphology of both the BHBN and cooked noodles samples were observed using scanning electron microscope (SEM) (Hitachi S-3400N, Shanghai Hitachi, China) at an operating voltage of 3.0 kV, as described by Yang et al.[9]. Samples preparation involved fixing a conductive adhesive tape onto a metal sample stage, mounting the sample onto the tape, and subjecting it to gold spraying. The morphological features of the samples were examined under a magnification of 500×.

2.3.2 Determination of the ordered structure of BHB starch

The BHBN and cooked BHBN samples were scanned with an X-ray diffractometer (D/Max2550, Rigaku, Japan)[10], Cu K_α radiation was used with a working voltage of 40 kV and a current of 100 mA, at a wavelength of 0.15 nm. The curves were fitted using a Gaussian function. The relative crystallinity of starch in the BHBN was calculated using MDI Jade 6.0 software (Materials Data, Inc., USA). The calculation formula for the relative crystallinity of starch is given by the equation (1).

$$\text{Relative crystallinity (\%)} = \frac{\text{Crystalline area}}{\text{Crystalline area + Diffraction area}} \times 100 \quad (1)$$

To prepare the samples for infrared spectroscopy, BHB starch samples and dried KBr powder were mixed in a ratio of 1/100 (sample/KBr). The mixture was ground into a powder in a mortar (Sinopharm Reagent Co., China) then placed into a mold. The sample was pressed into a transparent film using a tablet press at a pressure of 8 MPa. Attenuated total reflection (ATR) mode was used for testing, with a resolution of 4 cm^{-1} and a scanning range of 4 000−400 cm^{-1}.

2.3.3 Determination of starch particle size distribution in BHB

The BHB starch samples were ground into fine powder using a mortar and pestle, then sifted through a 100-mesh sieve. A total of 10 mg of noodle powder was added to 1 mL of distilled water and sonicated to ensure uniform mixing. The particle size distribution was measured using a laser particle size analyzer (Mastersizer 3000, Malvern, UK) in the range of 0.1−2 000.0 μm[11].

2.4 Evaluation of blood glucose-regulating effects of BHB in T2DM population

2.4.1 Study design

This study employed a randomized crossover design to allocate 30 participants into an experimental group and a control group using

a random number table[12]. The intervention period consisted of 3 stages, during which both groups received different interventions (Fig. 1). The experimental group was subjected to the BHBN2 intervention (BHBN Group). Firstly, the intervention group followed a regular dietary intervention (RD Group), while the control group followed the opposite sequence. The intervention frequency was 7 times per week, and each stage lasted for 2 weeks. The 1st and 3rd stages were intervention periods, while the 2nd served as a washout period. At the start of the intervention, both groups were provided with continuous glucose monitoring devices to record their blood glucose changes throughout the intervention period. Additionally, a 24-h dietary survey was conducted for 3 days during the intervention period. Blood and fecal samples were collected and stored during routine follow-up visits for subsequent analysis.

This study followed the principles outlined in the Helsinki Declaration (2013) and the Ethical Guidelines for Human Health-Related Research. Ethical approval for the involvement of human subjects was granted by the East China University of Science and Technology and Shanghai Chang Zheng Hospital Research Ethics Committee (reference number ECUST-2022-080, 2022SL061). The study was registered with the Chinese Clinical Trial Registry (ChiCTR2300068505). All participants provided informed consent to participate in the study.

2.4.2 *Study participants*

Participants of any gender, aged between 30−80 years, were recruited following inclusion and exclusion criteria. Participants were required to have a confirmed diagnosis of T2DM and an initial glycated hemoglobin (HbA1c) level of less than 9% on the first visit. Before enrolling, individuals had to maintain their medication regimen for the previous 3 months without any changes. Exclusion criteria included severe liver or kidney impairment, autoimmune diseases, malignancies, gastrointestinal disorders, conditions such as ketoacidosis or hyperosmolar hyperglycemia, and pregnancy or lactation for women. Participants were excluded from the study if they had consumed yogurt or fermented products during the experimental period, used antibiotics, probiotics, gastrointestinal motility medications, or other agents affecting gut microbiota within the past 3 months, had a history of serious mental illness within the past 6 months, poor compliance, alcohol dependency, or participated in other research projects within the previous 3 months.

2.4.3 *Determination of gastrointestinal peptides*

Serum samples were centrifuged (2 000 × *g*, 5 min, 4 °C) and the resulting supernatant were collected. Gastrointestinal peptide levels were measured using the glucagon-like peptide-1 (GLP-1), GLP-2, and gastric inhibitory peptides (GIP) enzyme-linked immunosorbent assay (ELISA) kits, following the provided instructions[13].

2.4.4 *Metabolism profiling of fecal metabolites*

Fecal samples were collected, and 60 mg of each sample was weighed into a 1.5 mL microcentrifuge tube. The fecal samples were pretreated according to the literature[14]. The resulting supernatant was transferred to LC-MS sample vials with footed inserts for analysis. The ACQUITY UPLC® HSS T3 (100 mm × 2.1 mm, 2.5 μm) chromatographic column was used.

The mobile phase A was composed of water with 0.1% formic acid (*V/V*), while the mobile phase B was composed of acetonitrile with 0.1% formic acid (*V/V*). The column temperature was 40 °C, flow rate was 0.35 mL/min, and sample injection volume was 2 μL. The mass spectrometry data in RAW format were aligned and identified for peak detection. Metabolites were matched against the spectral library of the Human Metabolome Database (HMDB). The resultant data were then imported into SIMCA 14.1 software (Umetrics AB, Sweden), with partial least squares discriminant analysis (PLS-DA) and orthogonal partial least squares discriminant analysis (OPLS-DA) subsequently applied for data visualization.

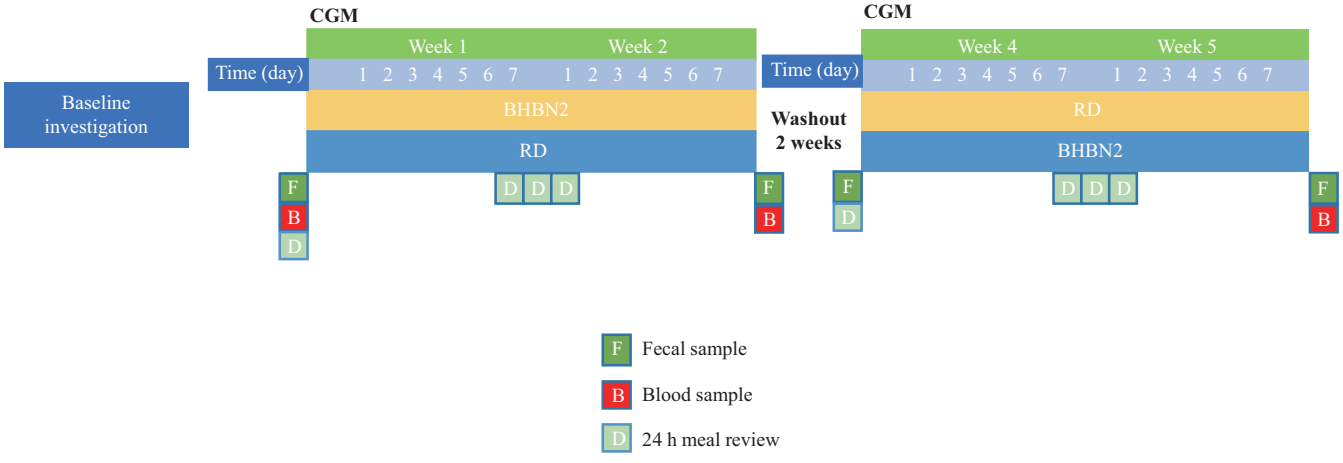

Fig. 1 Randomized crossover experimental procedure was conducted to study the effects of BHBN on the T2DM population.

2.4.5 Determination of relative abundance of gut microbiota

Fecal sample (60 mg) was placed in a 2 mL sterile centrifuge tube and washed with PBS to pellet the bacteria, and RNA from intestinal microorganisms was extracted[15]. The RNA concentration was normalized and then reverse transcribed to cDNA using the RNA reverse transcription kit and primer sequences designed based on references and primer design software instructions (Table S2). The fluorescence data were analyzed and processed using the appropriate software to calculate the abundance and trend changes.

2.5 In vitro dynamic digestion and glucose release kinetics of BHB

2.5.1 In vitro dynamic digestion of BHB starch

The electrolytes used in the simulation were prepared following the instructions in Table S3. To prepare the simulated saliva, 0.20 g of *α*-amylase was dissolved in 100 mL of the saliva electrolyte solution. The gastric fluid was prepared by dissolving 0.50 g of pepsin in 100 mL of the gastric electrolyte solution. The intestinal fluid was prepared by dissolving 1.80 g of pancreatin and 0.30 g of lipase in 100 mL of the intestinal electrolyte solution. Each 100 mL of simulated bile contained 6.00 g of bile salts and an electrolyte solution.

The beaker was placed in a constant temperature water bath at 37 °C to simulate oral digestion. After oral digestion, the digested noodles were poured into the funnel of a dynamic digestion model positioned above the esophagus. The duration of one digestion process was set to 2 h. Samples were collected at 15 min intervals from the gastric emptying port, and the volume and mass of the expelled solution were recorded for subsequent analysis[16].

2.5.2 Determination of BHBN digestion characteristics

Gastric emptying rate is the speed at which food passes from the stomach to the small intestine. The calculation formula was given in the equation (2). Based on the gastric emptying rate, the food retention in the stomach was calculated. The gastric emptying curve for BHBN was obtained by plotting food retention in the stomach against time. The equation for gastric emptying kinetics of BHBN was derived by fitting the improved Elashoff power exponential model[17], as shown in equation (3). The half-life ($t_{1/2}$) was calculated from the kinetic equation when $y(t) = 0.5$, using equation (4).

$$\text{Gastric emptying rate (\%)} = \frac{\text{The mass of digesta expelled from the stomach at time } t}{\text{Total mass of food}} \times 100 \quad (2)$$

$$y(t) = 1 - (1 - e^{-kt})^{\beta} \quad (3)$$

$$t_{1/2} = -\frac{1}{k} \times \ln\left(1 - 0.5^{\frac{1}{\beta}}\right) \quad (4)$$

Here, $y(t)$ represents the retention rate of food in the stomach, k is the emptying rate per minute, and β is the inferred curve intercept. The speed of gastric emptying was commonly described using the half-emptying time ($t_{1/2}$) of the stomach.

The glucose concentration in the collected digestive fluid was measured at different time points using the method specified in the glucose kit. Based on the calculated Gt results in Section 2.4.2, the starch hydrolysis rate was calculated using the equation (5).

$$\text{Starch hydrolysis rate (\%)} = \frac{\text{Gt} \times 0.9}{\text{TS}} \times 100 \quad (5)$$

Here, TS represents the total starch content, and 0.9 is the coefficient for starch conversion to glucose. The starch digestion curve was fitted using the non-linear first-order rate equation

$$C_t = C_{\infty}(1 - e^{-kt}) \quad (6)$$

Where C_t represents the amount of starch hydrolyzed at digestion time t, C_{∞} represents the amount of starch hydrolyzed at the end of digestion, and k is the first-order rate constant.

The hydrolysis index (HI) of the noodles is the ratio of the area under the hydrolysis curve of the noodles to the area under the hydrolysis curve of the standard food, white bread. The estimated GI values of BHBN are calculated using the formula proposed by Granfeldt et al.[18] in equation (7). At 0, 20, 60, and 120 min, 2 mL of digestive fluid were collected. Glucose concentration was measured using the method specified in the Glucose assay kit. The content of rapidly digestible starch (RDS), slowly digestible starch (SDS), and resistant starch (RS) were calculated using the following equations (8–10).

$$\text{eGI} = 0.862\text{HI} + 8.198\ 1 \quad (7)$$

$$\text{RDS (\%)} = \frac{(G_{20} - G_0) \times 0.9}{\text{TS}} \times 100 \quad (8)$$

$$\text{SDS (\%)} = \frac{(G_{120} - G_{20}) \times 0.9}{\text{TS}} \times 100 \quad (9)$$

$$\text{RS (\%)} = \frac{1 - \text{RDS (\%)} - \text{SDS (\%)} \times 0.9}{\text{TS}} \times 100 \quad (10)$$

Where, G_0 represents the glucose concentration without digestion; G_{20} represents the glucose concentration after 20 min of digestion; G_{120} represents the glucose concentration in the digestive solution after 120 min of digestion.

2.6 Statistical analysis

The data were presented as mean ± standard deviation (SD). Normality of data distribution was assessed by the Shapiro-Wilk test. Statistical analysis was performed using SPSS software (Version 2.1, IBM, USA), including one-way ANOVA and Duncan's multiple comparison analysis, to assess the differences in the data. The significance level of $P < 0.05$ was considered significant, and different letters were used to indicate significant differences.

3. Results and discussion

3.1 Microstructural analysis of BHB starch

3.1.1 Analysis of BHB starch microstructure

shown in Fig. S1A, wheat starch particles were round with a smooth surface. The particle size distribution was uneven, and the

particles were loosely packed, with small starch particles often adhering to the surface of larger ones. The starch particles in BHB were polygonal with a rough surface and central pores (Fig. S1B). They were uniformly distributed in size and tightly packed, forming agglomerates with multiple particles.

When wheat flour and BHB flour were used to make noodles, the morphology of the starch particles changed. Post-processing into WN, starch particles became sticky, with many small starch particles adhering to the surface (Fig. 2), due to the agglomeration of small starch particles into larger particles under the influence of moisture. The starch particles in the noodles made with a mixture of BHB and wheat flour were found to be more tightly connected and had fewer gaps on the surface compared to those made with wheat flour alone[4]. The addition of more BHB resulted in a gradual decrease in the contents of small starch particles on the surface. After ripening, the surfaces of BHBN2 and mixed-grain noodles appeared rough, and the intact starch particle morphology was still observable.

3.1.2 Analysis of BHB starch structure

X-ray diffraction analysis revealed characteristic peaks at 2θ = 15.2°, 17.5°, 18.0°, and 23.0° for WN, indicating a typical A-type crystal structure. BHBN1, BHBN2, and CN also exhibited characteristic peaks at 2θ = 15.2°, 17.5°, 18.0°, 20.0°, and 23.0° (Fig. 3A), with the peak at 2θ = 20.0° indicating a V-type crystal structure[19]. Therefore, WN had an A-type crystal structure, while BHBN1, BHBN2, and CN have an A + V-type crystal structure. Linear starch and various guest molecules form V-type crystals, and BHBN1, BHBN2, and CN had higher linear starch content and rich nutrient content, making them prone to complex formation and V-type crystal structure. After ripening, the crystal characteristic peaks almost disappeared. However, BHBN2 and CN still showed residual peaks at 2θ = 15.6° and 20.7° (Fig. 3B), indicating the presence of A-type and V-type crystal structures. These results indicated that the addition of BHB and mixed grains enhanced the long-range ordered structure of starch (Table 1), and with increasing BHB content, some

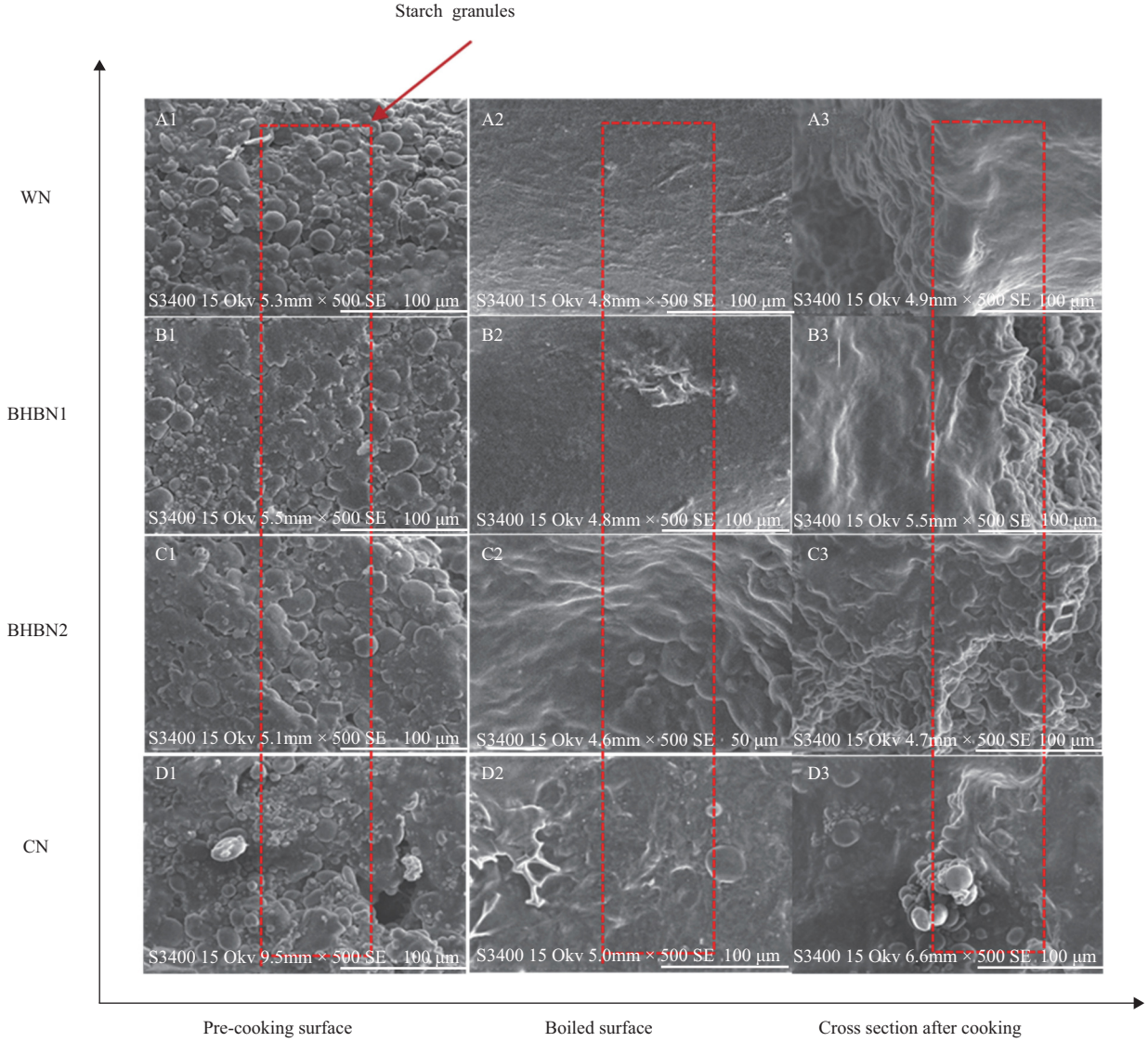

Fig. 2 Changes in the microscopic particle morphology of BHBN before and after cooking (500×). The horizontal axes were the surface of the BHBN before cooking, the surface after cooking, and the cross-section after cooking. The vertical axis showed different types of noodles. The red box showed the starch granules.

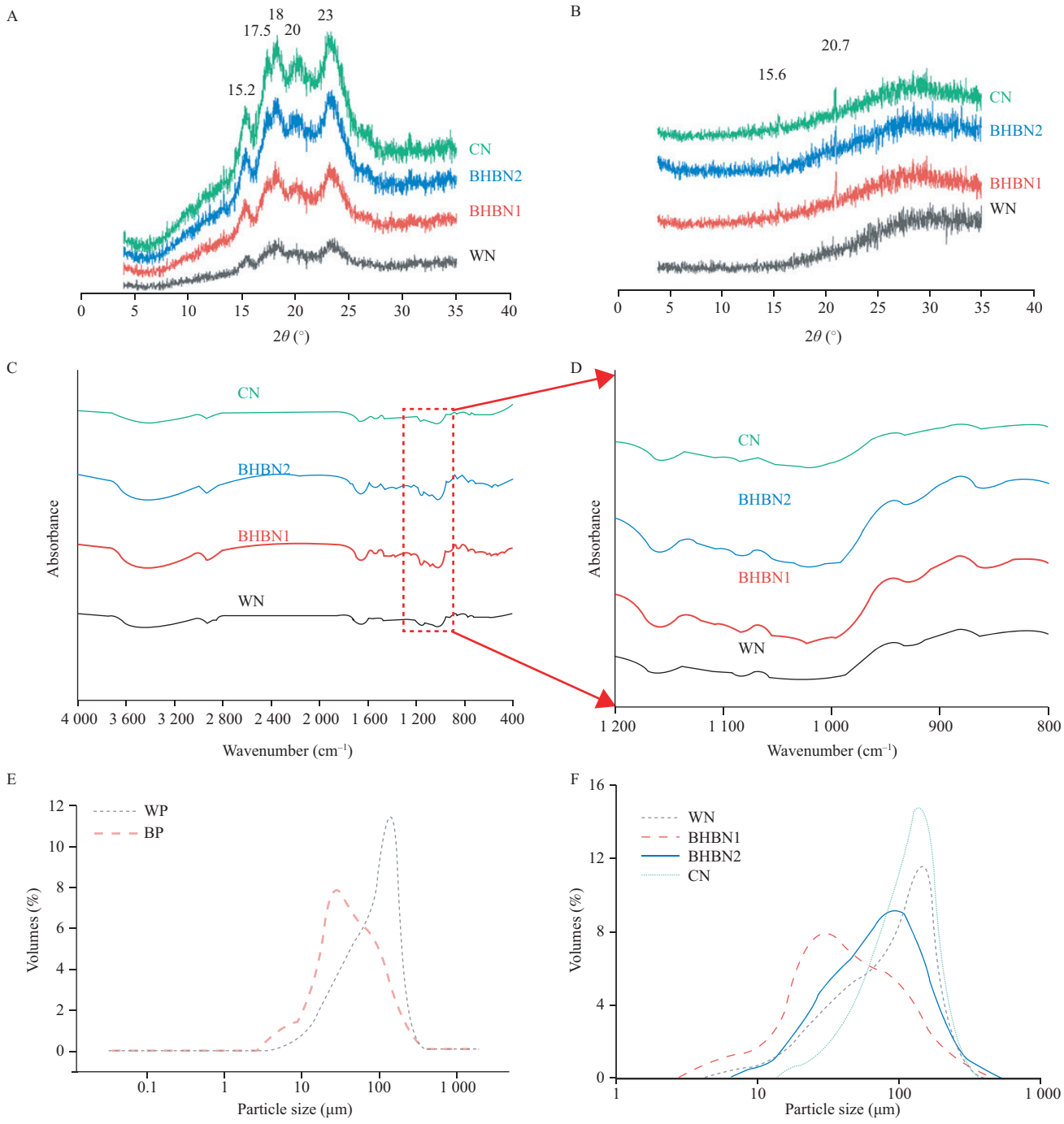

Fig. 3 Microstructural characterization of BHB starch. (A) Crystal structure of noodles before maturation. (B) Crystal structure of matured BHBN. (C) Attenuated total reflectance-fourier transform infrared spectroscopy (ATR-FTIR) spectrum of BHB starch in the 400−4 000 cm^{-1} range. (D) ATR-FTIR spectrum of BHB starch in the 800−1 200 cm^{-1} range. (E) Distribution of starch particle size. (F) Distribution of BHB starch particle size.

characteristic crystal peaks were retained after ripening. Fig. 3C represented the full-wavelength scan spectrum of the samples, with the spectral region of 800−1 200 cm^{-1} corresponding to the starch polymer (Fig. 3D).

The absorption peaks in this range were caused by the vibrations of C−C, C−O, and C−H−O bonds, and they are highly sensitive to the short-range ordered structure of starch[20]. The absorbance at 1 047 cm^{-1} was related to the crystalline region of starch, while the reflectance at 1 022 cm^{-1} corresponds to the amorphous region of starch, and the absorption peak at 995 cm^{-1} was mainly related to intramolecular hydrogen bonding of the C-6 hydroxyl group of starch. The absorbance ratio at 1 047/1 022 cm^{-1} and 1 022/995 cm^{-1} is commonly used to characterize the short-range ordered structure and double helix order of starch samples[21]. A higher ratio of absorbance at 1 047/1 022 cm^{-1} and a lower ratio of absorbance at 1 022/995 cm^{-1} indicated a higher degree of short-range ordered structure in starch.

Table 1
Relative crystallinity and short-range ordered structure of BHB starch.

Group	Initial relative crystallinity (%)	After maturation relative crystallinity (%)	1 047/1 022 cm^{-1}	1 022/995 cm^{-1}
WN	15.57 ± 0.01^{c}	2.32 ± 0.03^{d}	1.01 ± 0.06^{a}	0.86 ± 0.02^{a}
BHBN1	19.38 ± 0.38^{c}	3.55 ± 0.04^{c}	1.03 ± 0.05^{a}	0.74 ± 0.01^{b}
BHBN2	30.14 ± 1.05^{a}	7.88 ± 0.44^{a}	1.03 ± 0.04^{a}	0.73 ± 0.07^{b}
CN	26.54 ± 0.98^{b}	6.38 ± 0.28^{b}	1.01 ± 0.02^{a}	0.85 ± 0.04^{a}

Note: Data were expressed as mean ± SD. Lowercase letter labels in the same column indicated significant differences between groups ($P < 0.05$).

The relative crystallinity of BHB starch in the noodles was calculated by fitting the characteristic peaks of the X-ray diffraction spectra using Gaussian functions (Table 1). The relative crystallinity of BHBN1 was 19.38%, and BHBN2 had a relative crystallinity of 30.14%. Compared to WN, the relative crystallinity of the BHB group was significantly higher ($P < 0.05$). Compared to CN, BHBN1 showed a decrease of 7.16% in relative crystallinity, while BHBN2 showed an increase of 3.60% ($P < 0.05$).

The BHBN2 exhibited a higher relative crystallinity than CN, indicating a higher degree of long-range ordered structure. This result was consistent with the starch morphology structure characterized on the surface of the noodles before ripening (Fig. 2). After ripening, the crystal characteristic peaks nearly disappeared, and the relative crystallinity significantly decreased. The calculated relative crystallinity after ripening was 3.55% for BHBN1 and 7.88% for BHBN2. BHBN1 and BHBN2 with BHB starch addition had higher relative crystallinity after ripening compared to WN, and the relative crystallinity was positively correlated with the amount of barley added. Compared to CN, BHBN2 exhibited a higher relative crystallinity after ripening, indicating that BHBN2 retained more intact starch granule structures, indicating that the addition of BHB effectively preserved the integrity of some starch structures.

The infrared spectra of the four types of noodles were shown in Table 1. Both BHBN1 and BHBN2 had a value of 1.03 for the 1 047/1 022 cm^{-1} ratio. There was no statistical difference compared to the control groups WN and CN ($P > 0.05$). The value of 1 022/995 cm^{-1} for BHBN1 was 0.74, and for BHBN2, it was 0.73. These values were significantly lower than those of WN and CN ($P < 0.05$). The lower value of 1 022/995 cm^{-1} for BHBN1 and BHBN2 indicated a higher content of short-range ordered structures.

3.1.3 BHB starch particle size distribution analysis

Differences in particle size play a key role in the structure, porosity, specific surface area, and digestive functional properties of starch[22]. The distribution of starch particle size in WP and BP was determined (Fig. 3E). The starch particle size distribution in WP ranged from 4.63 to 296.00 μm. The largest volume proportion was occupied by starch particles with a diameter of 148.00 μm. This observation is consistent with the results of wheat starch (Fig. S1A), indicating that wheat flour contains both large and small starch granules, with many smaller granules adhering to the surface of larger ones. The starch granules in BP were evenly distributed, with a particle size distribution ranging from 3.27 to 418.60 μm. The highest volume proportion was occupied by starch particles with a diameter of 31.11 μm.

After making the noodles, the starch granules in BHBN1 and BHBN2 increased in size, and the peak of the particle size distribution shifted to around 100.00 μm. In contrast, the peak of the starch particle size distribution in WN shifted to 46.30 μm, which is consistent with the observation of starch granules in noodles under SEM. After the noodles were made, small starch particles agglomerated to form larger particles, resulting in a decrease in the number of small starch particles and a narrower peak width in the particle size distribution. The BHBN2 starch granules had a particle size distribution range of 12.00−491.00 μm, and a sharper distribution peak compared with those of WN, BHBN1, and CN groups. The particle size distribution trend in BHBN1 was similar to BHBN2. Compared to the control groups WN and CN, the BHBN groups had more large starch granules. The results indicated that the inclusion of BHB in noodles led to a denser starch structure and larger particle size, resulting in the reduced starch digestibility.

3.2 Assessing the glucose-regulating effects of BHBN in a randomized clinical trial among individuals with T2DM

3.2.1 Baseline characteristics analysis

Baseline data for this study were collected within the 2 weeks preceding the commencement of the experiment through questionnaire surveys and physical examinations (Table 2). It could be inferred that the characteristics of the 2 experimental groups were comparable before the start of the experiment ($P > 0.05$). Furthermore, the energy and major nutrient intake levels of both the experimental and control groups remained essentially consistent throughout the trial period, showing no significant differences ($P > 0.05$) (Fig. S2).

3.2.2 Effects of BHBN intervention on glycemic metabolism

Fasting blood glucose, combined with glycated hemoglobin, is an important indicator for the diagnosis of diabetes. During the first phase of the intervention with BHBN, the experimental group had an average fasting blood glucose level of 6.43 mmol/L and a glycated hemoglobin level of 6.55%. In the second phase, after resuming regular staple food, the average fasting blood glucose level increased to 6.69 mmol/L, while the glycated hemoglobin level decreased to 6.40%. For the control group, in the first phase, after maintaining their initial dietary habits, the average fasting blood glucose level was 6.80 mmol/L, and the glycated hemoglobin level was 6.72%. In the second phase, after the intervention with BHBN, the average fasting blood glucose level was 6.88 mmol/L, and the glycated hemoglobin level was 6.65%.

Table 2
Baseline characteristic analysis of population with T2DM.

Project	Experiment group (E) (n = 15)	Control group (C) (n = 15)	P
Age (year)	54.07 ± 9.83	57.46 ± 8.61	0.351
Weight (kg)	70.66 ± 9.10	68.74 ± 9.87	0.585
Height (cm)	166.40 ± 10.06	167.93 ± 7.41	0.638
Gender (male/female)	2/1	2/1	
BMI (kg/m^2)	25.30 ± 1.34	24.37 ± 1.64	0.122
Waist (cm)	88.43 ± 7.37	83.77 ±7 .01	0.086
Disease duration (year)	6.10 ± 5.31	5.62 ± 6.31	0.918
SBP (mmHg)	122.86 ± 6.10	125.75 ± 8.36	0.309
DBP (mmHg)	79.66 ± 4.80	80.84 ± 7.24	0.611
HR (times/min)	78.80 ± 8.81	75.93 ± 4.41	0.269
BFP (%)	30.60 ± 4.89	28.19 ± 4.29	0.955
ALT (U/L)	20.07±7.82	22.00 ± 10.02	0.575
AST (U/L)	22.31 ± 12.61	22.31 ± 12.61	0.600
AST/ALT	1.06 ± 0.31	1.05 ± 0.30	0.982
UA (μmol/L)	339.06 ± 129.88	321.78 ± 55.51	0.649
HbA1c (%)	6.71 ± 0.65	6.71 ± 0.98	0.994
FBG (mmol/L)	6.56 ± 1.11	6.79 ± 1.18	0.322
INS (mmol/L)	8.78 ± 2.88	8.35 ± 5.50	0.798
C-PR (mmol/L)	0.76 ± 0.24	0.66 ± 0.28	0.315
HOMA-IR	2.69 ± 0.85	2.68 ± 1.84	0.992
TC (mmol/L)	4.62 ± 1.15	4.21 ± 1.45	0.395
TG (mmol/L)	1.74 ± 1.24	2.07 ± 1.63	0.540
HDL-C (mmol/L)	1.31 ± 0.41	1.41 ± 0.27	0.452
LDL-C (mmol/L)	2.52 ± 1.07	2.33 ± 0.90	0.612
IL-6 (pg/mL)	＜1.50	＜1.50	
IL-10 (pg/mL)	＜5.00	＜5.00	
IL-1β (pg/mL)	＜5.00	＜5.00	
TNF-α (pg/mL)	7.20 ± 2.77	7.42 ± 2.51	0.823
CRP (mg/L)	1.38 ± 0.50	1.07 ± 0.26	0.053

Note: Data were expressed as mean ± SD. Statistical significance was considered at $P < 0.05$. BMI, body mass index; SBP, systolic blood pressure; DBP, diastolic blood pressure; HR, heart rate; BFP, body fat percentage; ALT, alanine aminotransferase; AST, aspartate aminotransferase; UA, uric acid; FBG, fasting blood glucose; INS, insulin; C-PR, C-peptide.

After the intervention with BHBN, both groups exhibited no significant differences in their fasting blood glucose and glycated hemoglobin levels compared to the baseline values. The hydrolysis of proinsulin can lead to the release of equimolar amounts of insulin and C-peptide. Therefore, C-peptide may better represent the real-time secretion of insulin and serve as a biomarker of insulin resistance and β-cell function[23]. The experimental group had an average fasting insulin level of 7.97 mmol/L after 2 weeks of BHBN intervention (Fig. S3). After a 2-week recovery period with RD, the average fasting insulin level was 9.23 mmol/L. During the first phase of the RD period, the control group had an average fasting insulin level of 10.99 mmol/L. In conclusion, consumption of BHBN improved glucose metabolism and induced insulin resistance.

3.2.3 Effects of BHBN intervention on blood glucose variability

The ambulatory glucose profile (AGP) is a graphical representation that overlays multiple days of blood glucose monitoring data onto a standard 24-h format[24]. Individuals with T2DM exhibit abnormal blood glucose fluctuations, characterized by 3 distinct "bread peaks" and significant postprandial blood glucose changes. Fasting blood glucose and glycated hemoglobin cannot reflect blood glucose variability or quantify the amplitude and variability of blood glucose fluctuations throughout the day. CGM, which monitors blood glucose levels throughout the entire duration, can effectively compensate for the limitations of these 2 important indicators and quantify blood glucose variability. During the intervention and recovery phases with regular staple food, CGM was used to monitor the participants' blood glucose changes (Fig. 4). During the BHB intervention phase, most participants' AGP profiles showed a reduction in one of the "bread peaks", which reappeared after the resumption of RD.

The coefficient of variation (CV) was a parameter of blood glucose variability, representing the average daily blood glucose fluctuation throughout the monitoring period. The experimental group had an average CV value of 23.31% during the BHBN intervention phase and 24.88% during the recovery phase (Table 3). Comparing these 2 stages, the consumption of BHBN resulted in a 1.57% reduction in CV value. For the control group, the average CV value during the RD phase was 26.82%. During the BHBN intervention phase, the average the CV value decreased to 25.55%. The results were consistent with the experimental group, showing a 1.27% reduction in CV value due to the intervention of BHBN. Mean amplitude of glycemic excursions (MAGE) describes the extent of blood glucose fluctuations throughout the day and is calculated by subtracting the minimum blood glucose value from the maximum value on a given day. During the BHBN intervention phase, the experimental group had a MAGE level of 3.81 mmol/L. During the recovery phase, the MAGE level increased to 4.04 mmol/L. The MAGE value during the BHBN intervention phase was 0.23 mmol/L lower than that during the recovery phase. For the control group, the MAGE value during the recovery phase was 4.53 mmol/L, while during the BHBN intervention phase, it was 3.92 mmol/L, indicating a reduction of 0.61 mmol/L compared to the recovery phase. Both CV value and MAGE were indicators of blood glucose variability. Data from both groups reveals that the consumption of BHBN can reduce blood glucose variability.

3.2.4 Effects of BHBN intervention on gastrointestinal peptides and gut microorganisms

The nutritional substances in noodles are primarily absorbed in the small intestine. GIP in the small intestine respond to the release of

Table 3
Changes in blood glucose related indicators in T2DM population.

Project	E-BHBN	E-RD	C-RD	C-BHBN
Predicted glycated hemoglobin (%)	5.97 ± 1.01^a	5.86 ± 0.72^a	6.71 ± 1.31^a	6.57 ± 1.32^a
Mean glucose value (mmol/L)	6.57 ± 1.19^a	6.44 ± 0.86^a	7.46 ± 1.57^a	7.29 ± 1.58^a
Mean glucose fluctuation, MAGE (mmol/L)	3.81 ± 0.11^b	4.04 ± 0.51^b	4.53 ± 0.25^a	3.92 ± 0.40^b
CV (%)	23.31 ± 5.04^a	24.88 ± 6.29^a	26.82 ± 5.51^a	25.55 ± 5.35^a
Glucose SD (mmol/L)	1.67 ± 0.71^a	1.53 ± 0.50^a	2.03 ± 0.71^a	1.89 ± 0.66^a

Note: Data were expressed as mean ± SD. Lowercase letter labels in the same row indicated significant differences between groups ($P < 0.05$). E-BHBN, black barley intervention phase for the group that received black barley intervention first; E-RD, RD phase for the group that received black barley intervention first. C-BHBN, black barley intervention phase for the group that received RD first; C-RD, RD phase for the group that received RD first.

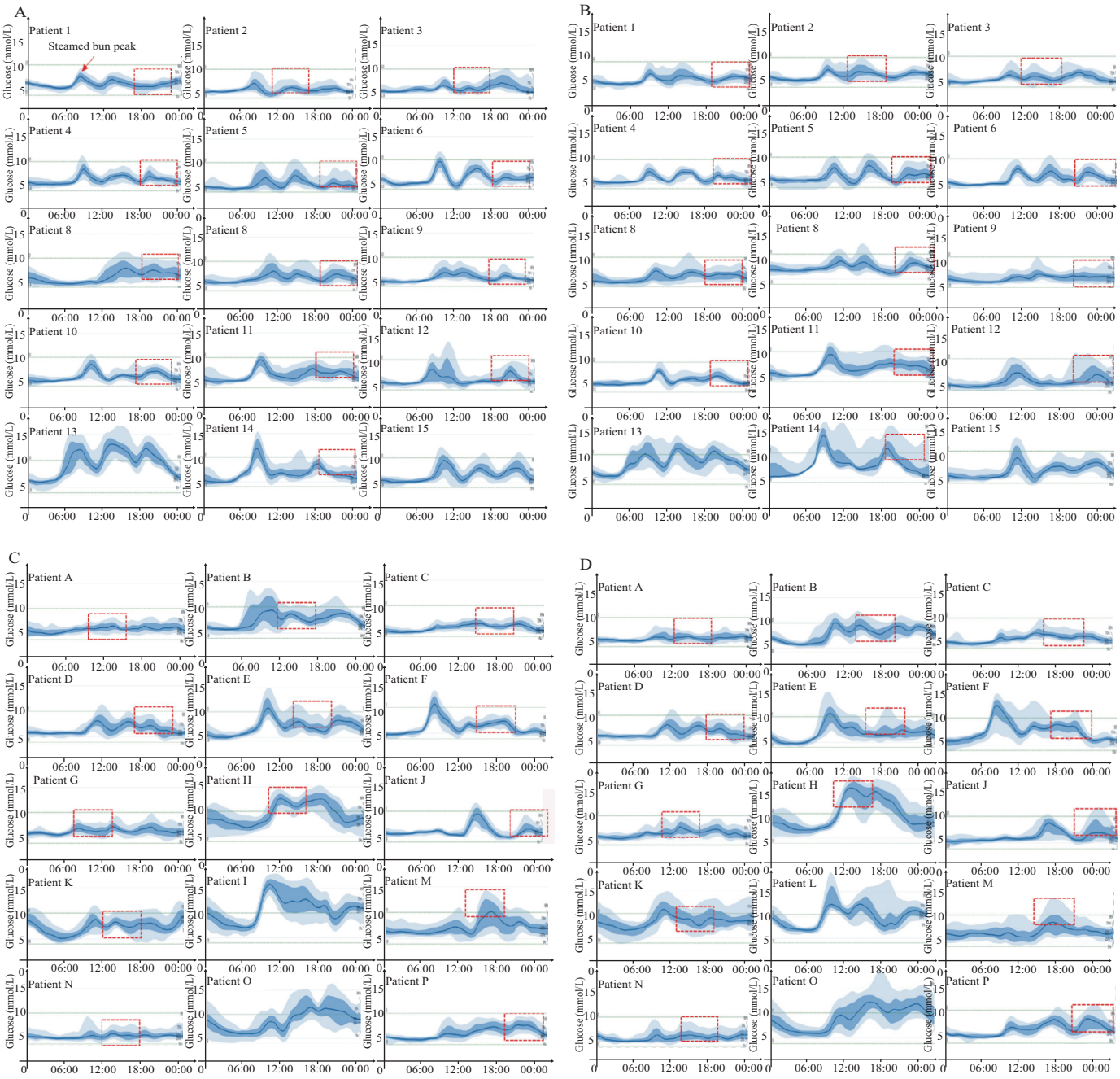

Fig. 4 Dynamic glucose profiles in subjects with T2DM individuals. (A) The 24-h dynamic glucose profiles of the population in the C-BHBN group. (B) Dynamic glucose variations in the C-RD group. (C) Dynamic glucose profiles of the E-BHBN group. (D) Dynamic glucose variations in the E-RD group. Each dynamic glucose profile was a 14-day cumulative profile of blood glucose values. The horizontal axis was 24 h for the whole day, the vertical axis was the glucose concentration. The patients in panels A and B were from the same cohort, panels C and D were from the same cohort. The red boxes showed the peaks in blood glucose fluctuations.

nutrients, promoting insulin production and secretion while inhibiting glucagon secretion[25]. GLP-1 slows gastric emptying through the vagus nerve and GLP-2 is an intestinal epithelial growth factor that promotes intestinal growth and mucosal repair, maintaining and enhancing intestinal barrier integrity[26]. The levels of gastric inhibitory peptides GLP-1, GLP-2, and GIP were measured (Fig. 5).

Following BHBN intervention, the GLP-1 level for the experimental group remained stable at 7.96 pmol/L, which was similar to the baseline value of 7.80 pmol/L. During the recovery phase, the GLP-1 level for the experimental group was 8.09 pmol/L, showing no significant difference from the baseline data. The control group had a baseline GLP-1 level of 7.87 pmol/L. In the first phase with no dietary changes, the average GLP-1 level was 8.04 pmol/L, indicating a 0.17 pmol/L increase compared to the baseline. After a 2-week BHBN intervention, the mean GLP-1 concentration increased to 8.29 pmol/L, which is a 0.42 pmol/L increment from the baseline measurement. The experimental group exhibited a GLP-2 level of 13.11 pmol/L at baseline. Following the BHBN intervention, it increased to 13.57 pmol/L, which is a 0.46 pmol/L increase from the baseline. During the recovery period, the GLP-2 level increased by 0.38 pmol/L compared to the baseline, measuring 13.49 pmol/L.

For the control group, the baseline GLP-2 level was 13.11 pmol/L. During the first phase, the GLP-2 level slightly decreased to 12.95 pmol/L. After 2 weeks of BHBN intervention in the second phase, the GLP-2 level significantly increased compared to the baseline. GIP stimulated glucagon secretion, enhanced gluconeogenesis and glycogenolysis, increased blood glucose levels. Lowering GIP levels is important for maintaining lower blood glucose levels. GIP significantly decreased after BHBN intervention ($P < 0.05$), with a decrease of 0.382 μg/L for the experimental group and a decrease of 0.16 μg/L for the control group. Therefore, the BHBN lower GIP levels and increase GLP-2 content. This plays a role in lowering blood glucose levels in situations of hyperglycemia and maintaining and enhancing intestinal barrier integrity, effectively relieving hyperglycemia. In the intestines of individuals with T2DM, probiotics such as *Akkermansia*, *Bifidobacterium*, and *Lactobacillus* have lower abundances, which can inhibit chronic inflammation and autoimmune diseases[27]. *Akkermansia*, when degrading mucin, produces acetate and propionate, and its abundance is strongly negatively correlated with blood glucose and inflammatory factors[28]. *Bifidobacterium* prevents or delays the onset of diabetes by repairing the intestinal barrier, inhibiting inflammatory reactions, reducing oxidative stress, restoring energy metabolism, and producing beneficial microbial metabolites (including SCFAs and bile acids)[29]. After BHBN intervention (Fig. 5), the relative abundance of *Akkermansia*, *Bifidobacterium*, and *Lactobacillus* significantly increased ($P < 0.05$). It can be attributed to that the indigestible components in BHBN provide available substrates for the probiotics in the lower digestive tract. These probiotics secrete SCFAs that bind to GPR41/43 receptors, promoting the secretion and release of gastrointestinal peptides such as GLP-1, and regulating blood glucose levels by increasing insulin secretion[30]. Although *Akkermansia*, *Bifidobacterium*, and *Lactobacillus* were demonstrated to be significantly correlated with glycemic homeostasis in this study, the relevance of changes in structural and functional microorganisms of the intestinal microflora induced by barley starch to glycemic regulation requires further investigation.

3.2.5 *Effects of BHBN intervention on differential fecal metabolites in T2DM individuals*

The partial least squares discriminant analysis (PLS-DA) and orthogonal partial least squares discriminant analysis (OPLS-DA) models were used to cluster the samples from the experimental and control groups in the positive and negative ion modes. In the positive ion mode, the samples within the same group were closely grouped but significantly separated under BHBN intervention and during the

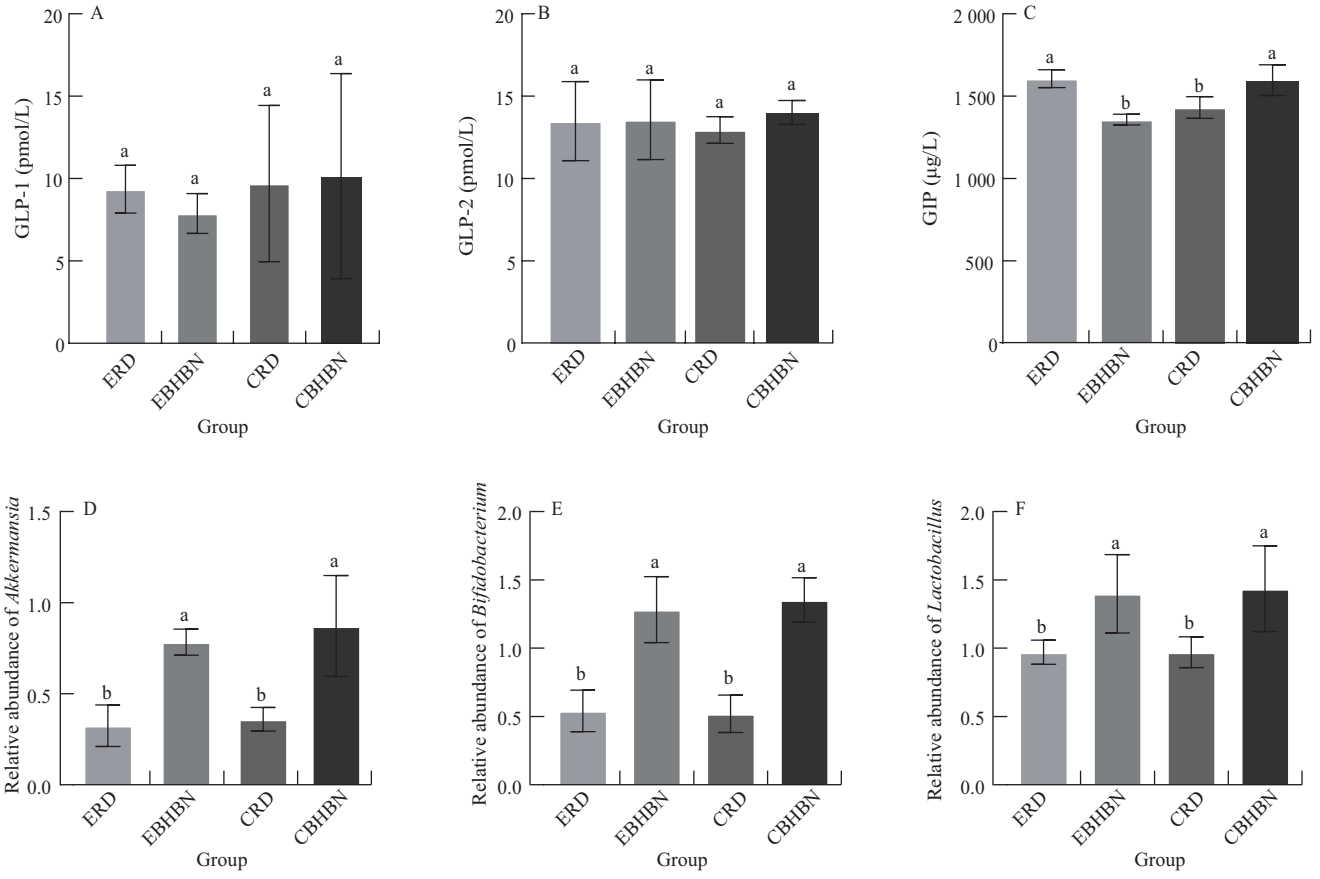

Fig. 5 Effect of BHBN intervention on gastrointestinal peptides and gut microorganisms. Levels of (A) GLP-1, (B) GLP-2, (C) GIP. Relative abundance of (D) *Akkermansia*, (E) *Bifidobacterium*, (F) *Lactobacillus*. Lowercase letter indicated significant differences between groups ($P < 0.05$).

recovery period. In the negative ion mode, the samples showed a similar trend under both measures (Figs. 6A-D). The results indicated that replacing staple foods with BHBN could alter gut metabolism. According to the criteria (Fig. S4), it indicated that the models were reliable. Therefore, the OPLS-DA model was selected to analyze differential metabolites in the gut due to the more compact sample points, indicating better clustering.

In the positive ion mode, before and after the intervention of BHB, there were a total of 3 typical metabolites that were upregulated and 2 metabolites were downregulated. Additionally, 2 metabolites showed no significant change (Table S4 and Fig. 6E). The upregulated metabolites were 7-hydroxycoumarinyl-*γ*-linolenate (MT08906), *N*-acetyl-*L*-2-aminoadipate (2-) (MT01351), and 4-hydroxycinnamyl aldehyde (MT04223). The downregulated metabolites were glycocholic acid (MT10371) and deoxycholic acid glycine conjugate (MT11298). The metabolites that showed no significant change were mesobilirubinogen (MT11411) and urobilinogen (MT08492). *N*-acetyl-*L*-2-aminoadipate (2-) is an intermediate metabolite of lysine metabolism, and it has been found to be higher in T2DM patients, making it a potential biomarker for T2DM[31]. Treatment of diet-induced obese mice with *N*-acetyl-*L*-2-aminoadipate has been shown to significantly reduce body weight, decrease fat accumulation, and lower fasting blood glucose levels by regulating insulin, making it a potential regulator of glucose homeostasis[32]. The upregulation of *N*-acetyl-*L*-2-aminoadipate (2-) was related to the reduction in glycemic variability. 4-hydroxycinnamyl aldehyde is an important intermediate in secondary metabolic pathways, whose derivatives serve as dietary antioxidants that have significant effects on immune

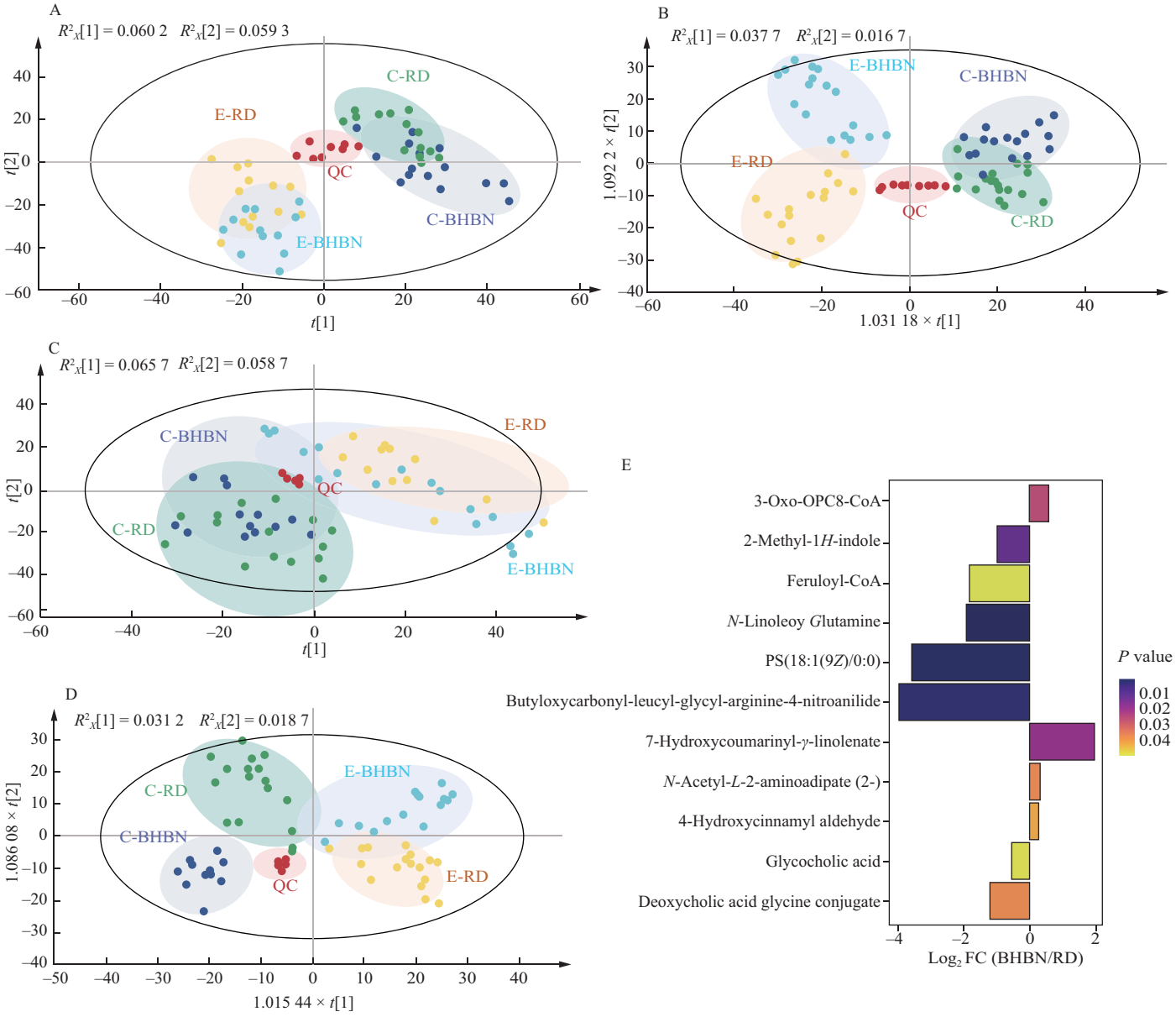

Fig. 6 Fecal differential metabolites of BHBN intervention were analyzed using cluster analysis and heatmap in positive and negative ion models ($n = 30$). (A) Cluster analysis based on PLS-DA model in positive ion mode. (B) Cluster analysis based on OPLS-DA model in positive ion mode. (C) Cluster analysis based on PLS-DA model in negative ion mode. (D) Cluster analysis based on OPLS-DA model in negative ion mode. (E) Typical differential intestinal metabolites after BHBN intervention compared with RD.

function[33]. Bilirubin is an effective endogenous antioxidant, and the total bilirubin in the body is negatively correlated with the incidence and progression of diabetic nephropathy. Urobilinogen is a product of bilirubin breakdown by intestinal bacteria[34]. The lack of significant changes in these 2 metabolites indicates that the disease state of the T2DM subjects remained relatively stable during the intervention. Bile acids and their derivatives are steroid signaling molecules that co-regulate metabolism and inflammation through farnesoid X receptor (FXR) and takeda G-protein coupled receptor 5 (TGR5)[35]. Glycocholic acid and deoxycholic acid glycine conjugate are positively correlated with insulin resistance[36], and the downregulation of these 2 metabolites may indicate relief of insulin resistance.

In the negative ion mode, the metabolite 3-oxo-opc8-CoA (MT02172) was found to be upregulated, while four other metabolites, namely feruloyl-CoA (MT00153), *N*-linoleoyl glutamine (MT06372), lysoPS (18:1(9*Z*)/0:0) (MT05693), and butyloxycarbonyl-leucyl-glycyl-arginine-4-nitroanilide (MT05697), were downregulated before and after BHB intervention (Table S5, Fig. 6E). 3-Oxo-opc8-CoA is a derivative of 3-oxoacyl-CoA, which converts long-chain fatty acids such as 3*α*,7*α*,12*α*-trihydroxy-5*β*-cholestanate into primary bile acid[37]. Bile acid circulates in the liver and intestines, aiding in the digestion and absorption of lipids in the small intestine and the excretion of cholesterol. The upregulation of 3-oxo-opc8-CoA indicates increased metabolism of primary bile acids. Feruloyl-CoA is involved in the production of vanillin from ferulic acid[38], and *Pseudomonas aeruginosa* is the major microorganism responsible for the conversion of ferulic acid to vanillin[39]. The downregulation of feruloyl-CoA is attributed to the intervention of BHB, which restores intestinal microbial homeostasis and reduces the abundance of *P. aeruginosa*. *N*-Linoleoyl glutamine is a long-chain *N*-acyl amide characterized as a transient receptor potential (TRP) channel antagonist[40]. Its elevation is positively correlated with impaired glucose tolerance, and the downregulation of *N*-linoleoyl glutamine may be related to the reparative effect of BHB intervention on impaired glucose tolerance. T2DM often accompanies lipid metabolism disorders. LysoPS (18:1(9*Z*)/0:0) is a glycerophospholipid that significantly increases in inflammatory bowel disease, such as Crohn's disease[41]. High levels of LysoPS (18:1(9*Z*)/0:0) accelerate intestinal inflammation. The downregulation of LysoPS (18:1(9*Z*)/0:0) in this study may indicate an alleviating effect on intestinal inflammation. In conclusion, the consumption of BHBN appears to modulate the gut metabolism of individuals with T2DM, which could contribute to regulating blood glucose homeostasis.

3.3 In vitro dynamic digestion analysis and glucose release pattern of BHBN

3.3.1 Gastric emptying during pasta digestion

Gastric emptying is a critical step in the food digestion process. In the stomach, food undergoes physical and chemical breakdown to form chyme, which is then emptied into the duodenum for further digestion and absorption. The rate of gastric emptying of BHBN is a crucial factor in postprandial blood glucose levels and is essential for maintaining blood glucose homeostasis[42]. As shown in Fig. 7A, the emptying trends of BHB and the other types of noodles were similar. The BHBN empty slowly during the first 0−30 min, followed by a linear rapid emptying phase in 30−75 min. After 75 min, the emptying rate slowed down, and by 120 min, almost complete emptying occurs. The Elashoff power exponential model fitting curves were shown in Fig. 7B, and the gastric emptying kinetics equations for WN, BHBN1, BHBN2, and CN were obtained as follows:

$$y = 1 - (1 - e^{-0.038x})^{4.989} \ (R^2 = 0.990) \quad (11)$$

$$y = 1 - (1 - e^{-0.038x})^{6.550} \ (R^2 = 0.990) \quad (12)$$

$$y = 1 - (1 - e^{-0.038x})^{7.125} \ (R^2 = 0.997) \quad (13)$$

$$y = 1 - (1 - e^{-0.038x})^{6.229} \ (R^2 = 0.997) \quad (14)$$

The gastric emptying parameters (Figs. 7A and B, Tables S6 and S7) indicated the presence of a retention period in the early stage of digestion, followed by a linear rapid emptying phase in the later stage. The parameters β obtained from the equations, all greater than 1, also indicate a significant lag in the initial stages of noodle digestion. The time required to empty 50% of the ingested contents ($t_{1/2}$) was commonly used to describe the speed of gastric emptying. The gastric half-emptying times for the 4 types of noodles were calculated to be 54.17, 61.02, 65.22, and 61.86 min, respectively. A shorter half-emptying time corresponds to a faster rate of emptying. Compared to WN, the gastric half-emptying time for the BHBN group significantly increased. BHBN1 had a 6.85 min longer half-emptying time than WN, while BHBN2 had an 11.04 min longer half-emptying time than WN. Compared to CN, there was no statistically significant difference in the gastric half-emptying time between BHBN1 and CN ($P > 0.05$). However, BHBN2 had a significantly longer half-emptying time than CN, with a difference of 3.36 min ($P < 0.05$). These results indicated that the addition of BHB starch slowed down the gastric emptying rate of BHBN.

3.3.2 Glucose release pattern during the digestion of BHB starch

The glucose concentration curves during digestion were shown in Fig. 7C and Table S8. The glucose concentrations of BHB and other types of noodles reached their peaks at 30 min into digestion and then continuously decreased afterward. Compared to WN, the glucose concentration in the digesta of BHBN1 was higher than WN from 0−45 min of digestion but lower than WN after 45 min. The intact gluten structure in WN might have hindered starch dissolution in the early stages of digestion. However, the more complete destruction of the WN structure in the later stages allowed for more complete starch digestion. At 30 min of digestion, the glucose in BHBN2 was significantly lower than WN ($P < 0.05$). During the 30−60 min period, BHBN2 exhibited a delay in glucose release compared to WN, resulting in a higher glucose concentration. BHBN1 had higher glucose concentrations at each time point compared to CN, while BHBN2 showed a similar glucose concentration curve to CN. As digestion time increases, the amount of released glucose continuously increased in BHBN group (Fig. 7D). The BHBN and other types of noodles exhibited similar patterns of glucose release: a linear increase

in glucose release rate in 0−30 min, followed by a slower rate and a flattening curve after 90 min of digestion. The mass emptying curve of WN was located above the other 3 curves, indicating a faster glucose release rate. The final amounts of glucose released in BHBN1, BHBN2, and CN, with the addition of BHB or whole grains, were all lower than that of WN, possibly due to their higher content of ordered structures.

3.3.3 *Hydrolysis rates and digestion kinetic curves of BHB starch*

The hydrolysis trend of BHB starch in the 2 types of noodles was generally consistent. Different crystal forms of starch had different hydrolysis and glucose release mechanisms and release kinetics. In the first 30 min of digestion, the starch hydrolysis rate showed a linear increase, followed by a decrease in the rate after 30 min, with a slow increase in the hydrolysis rate. The starch hydrolysis rate in WN was significantly higher than that in BHBN1, BHBN2, and CN ($P < 0.05$) (Fig. 7E, Table S9). After digestion, the starch hydrolysis rates for WN, BHBN1, BHBN2, and CN were 67.41%, 59.32%, 56.09%, and 59.59%, respectively. The starch hydrolysis rate in the BHBN group was significantly lower than that of WN ($P < 0.05$). Additionally, the results indicated a positive correlation between the starch digestion rate and the addition of BHB. Compared to WN, BHBN exhibited a lower starch digestion rate due to its higher dietary fiber content and proportion of amylose, as well as the presence of intact starch granule structures and a higher degree of ordered structures. Compared with to CN, BHBN had similar structures and component contents. However, BHBN2 had higher structural integrity and insoluble components than CN, which was consistent with the results of starch digestion rate. To describe the digestion kinetics of starch objectively, a first-order nonlinear equation $C_t = C_\infty(1 - e^{-kt})$ was used to fit the starch hydrolysis rate (Fig. 7F). This resulted in the digestion kinetic equation for BHB starch. The correlation coefficient R^2 of the fitted curves was close to 1, indicating that the digestion of starch in noodles followed the first-order kinetic equation for starch hydrolyzed at the end of digestion. The values obtained for starch hydrolyzed were 0.755, 0.663, 0.650, and 0.699, respectively, which were consistent with the results of the starch hydrolysis in noodles.

$$C_t = 0.755\ (1 - e^{-0.017t})\ (R^2 = 0.992) \quad (15)$$

$$C_t = 0.663\ (1 - e^{-0.017t})\ (R^2 = 0.994) \quad (16)$$

$$C_t = 0.650\ (1 - e^{-0.016t})\ (R^2 = 0.997) \quad (17)$$

$$C_t = 0.699\ (1 - e^{-0.015t})\ (R^2 = 0.995) \quad (18)$$

3.3.4 *Determination of estimated GI values*

The percentage of starch at different digestion rates is a determinant of starch digestion[43]. The RDS content in WN was 73.12%, SDS content was 12.14%, and RS content was 15.3% (Table 4). In BHBN1 group, RDS content was 63.24%, SDS content was 19.34%, and RS content was 17.5%. In BHBN2 group, RDS content was 59.29%, SDS content was 21.87%, and RS content was 19.2%. Compared to WN, the addition of BHB and mixed grains decreased the RDS content and increased the SDS and RS contents. Compared to

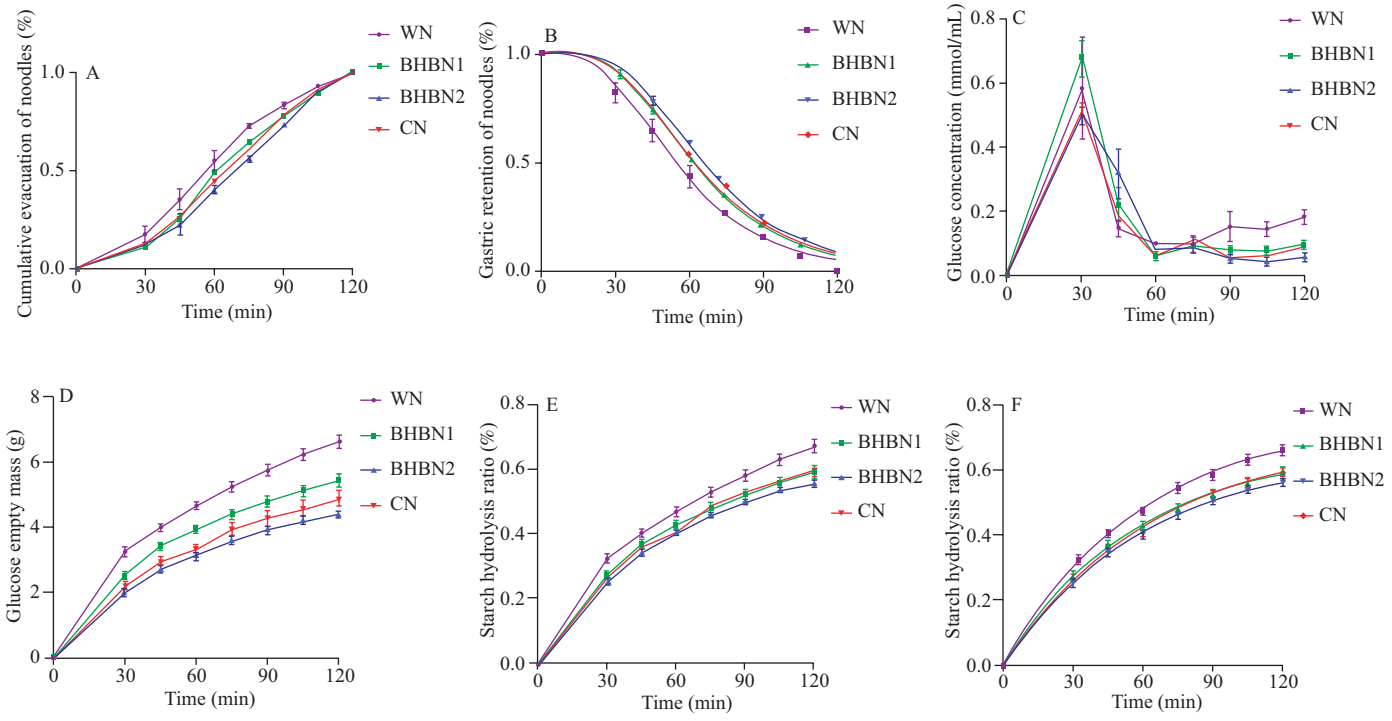

Fig. 7 Digestion kinetics curve of simulated BHBN was analyzed using a human dynamic digestion model. (A) Changes in gastric emptying rate. (B) Fitted curve of gastric emptying kinetics. (C) Changes in glucose concentration. (D) Cumulative glucose emptying mass curve. (E) Changes in hydrolysis rate of BHB starch. (F) Fitted curve of digestion kinetics of BHB starch.

CN, the addition of 70% BHB significantly reduced the RDS content in BHBN2, significantly increased the SDS and RS contents, while the addition of 30% BHB significantly increased the SDS content in BHBN1. The RDS content in BHBN1 was significantly higher than CN, while the RS content was significantly lower than CN. HI was the ratio of the area under the starch hydrolysis curve of noodles to that of white bread, and it could be used to estimate the eGI value of noodles. The eGI value of WN was 77.24, indicating a high GI-food. The eGI values of BHBN1, BHBN2, and CN were 54.73, 45.23, and 53.21, respectively, which are low GI-foods. In the BHBN group, the eGI value was negatively correlated with the addition of BHB. The addition of BHB and mixed grains reduced the GI of noodles. GI was an indicator of the magnitude of the postprandial blood glucose response, where RDS could cause a higher postprandial blood glucose response, and its content was positively correlated with GI. SDS and RS resulted in a lower glucose response, and their content was negatively correlated with GI. The addition of BHB increased the SDS and RS content, and decreased the blood glucose response, making it suitable for consumption by diabetics.

Table 4
Determination of starch content and estimated GI values of BHBN with different digestibility.

Group	RDS (%)	SDS (%)	RS (%)	HI	eGI
WN	73.12 ± 0.12^{d}	12.14 ± 0.04^{a}	15.3 ± 0.10^{a}	80.09 ± 1.27^{c}	77.24 ± 2.32^{c}
BHBN1	63.24 ± 0.08^{c}	19.34 ± 0.07^{c}	17.5 ± 0.03^{b}	53.98 ± 1.11^{b}	54.73 ± 1.46^{b}
BHBN2	59.29 ± 0.11^{a}	21.87 ± 0.19^{d}	19.2 ± 0.13^{c}	42.96 ± 2.15^{a}	45.23 ± 2.04^{a}
CN	61.21 ± 0.03^{b}	18.66 ± 0.03^{b}	18.9 ± 0.26^{c}	52.22 ± 0.79^{b}	53.21 ± 1.08^{b}

Note: Data were expressed as mean ± SD. Lowercase letter labels in the same column indicated significant differences between groups ($P < 0.05$).

4. Conclusion

This study employed a multifaceted approach, including population-based studies, *in vitro* digestion simulation, and mathematical model fitting, to elucidate the regulatory mechanism underlying blood glucose homeostasis induced by the anti-digestive effect of BHB on starch structural properties. The study found that the addition of BHB increased the size of starch granules and transformed the crystalline structure to an A + V type, resulting in a more organized structural arrangement compared to traditional WN. This study found that the structural alteration allowed for sustained glucose release after digestion. In 6-week population-based trials, BHB was shown to significantly reduce the CV in blood glucose and levels of ghrelin in individuals with T2DM, while also improving insulin resistance. Additionally, BHB intervention resulted in a significant increase in beneficial gut bacteria and an overall enhancement in non-targeted gut metabolites. To analyze the mechanism of BHB starch on blood glucose homeostasis and glucose release, a dynamic digestion protocol and mathematical model tailored specifically for BHB were developed. The gastric emptying kinetics of BHB, fitted to the Elashoff power exponential model, indicate that its slow gastric emptying and glucose release rates are pivotal factors contributing to its ability to maintain blood glucose stability. This study investigated the effect of BHB starch structure on sustained glucose release, providing a dietary strategy for managing blood glucose fluctuations in individuals with T2DM. Future research will focus on understanding how BHB modulates gut microbiota structure by influencing glucose release, which can improve dysbiosis in the intestinal microecology of T2DM populations. Additionally, efforts will be directed towards refining the formulation of BHB-enriched noodles using a microbiota-targeted approach tailored specifically for individuals with T2DM.

Acknowledgement

This work was supported by the Shanghai Sailing Program (23YF1409800), Natural Science Foundation of Shanghai (23ZR1415400) and Shanghai Frontiers Science Center of Optogenetic Techniques for Cell Metabolism (Shanghai Municipal Education Commission).

Conflict of interests

The authors declare that there are no conflict of intreset.

Appendix A. Supplementary data

Supplementary data associated with this article can be found, in the online version, at http://doi.org/10.26599/FSHW.2024.9250390.

References

[1] J. Liu, M. Liu, Z. Chai, et al., Projected rapid growth in diabetes disease burden and economic burden in China: a spatio-temporal study from 2020 to 2030, Lancet Reg. Health West Pac. 33 (2023) 100700. https://doi.org/10.1016/j.lanwpc.2023.100700.

[2] H. Toplak, F. Hoppichler, T.C. Wascher, et al., Obesity and type 2 diabetes, Wien. Klin. Wochenschr. 128 (2016) 196-200. https://doi.org/10.1007/s00508-016-0986-9.

[3] K. Esposito, P. Chiodini, M.I. Maiorino, et al., Which diet for prevention of type 2 diabetes? A meta-analysis of prospective studies, Endocrine 47 (2014) 107-116. https://doi.org/10.1007/s12020-014-0264-4.

[4] S. Liu, H. Liu, S. Gao, et al., Dry heating affects the multi-structures, physicochemical properties, and *in vitro* digestibility of blue highland barley starch, Front. Nutr. 10 (2023) 1191391. https://doi.org/10.3389/fnut.2023.1191391.

[5] C. Lu, Z. Zhao, G. Huang, et al., The contribution of cell wall integrity to gastric emptying and *in vitro* starch digestibility and fermentation performance of highland barley foods, Food Res. Int. 169 (2023) 112912. https://doi.org/10.1016/j.foodres.2023.112912.

[6] Y. Lü, S. Ma, J. Yan, et al., Effect of heat–moisture treatment on the physicochemical properties, structure, morphology, and starch digestibility of highland barley (*Hordeum vulgare* L. var. nudum Hook. f) flour, Foods 11(21) (2022) 3511. https://doi.org/10.3390/foods11213511.

[7] L. Y. Liu, X.Y. Wang, Y. Li, et al., Postprandial differences in the amino acid and biogenic amines profiles of impaired fasting glucose individuals after intake of highland barley, Nutrients 7(7) (2015) 5556-5571. https://doi.org/10.3390/nu7075238.

[8] F.Y. Liu, X.N. Guo, J.J. Xing, et al., Effect of thermal treatments on *in vitro* starch digestibility of sorghum dried noodles, Food Funct. 11(4) (2020) 3420-3431. https://doi.org/10.1039/C9FO02765C.

[9] Y. Yang, A. Jiao, Q. Liu, et al., The effects of removing endogenous proteins, *β*-glucan and lipids on the surface microstructure, water migration and glucose diffusion *in vitro* of starch in highland barley flour, Food Hydrocoll. 127 (2022) 107457. https://doi.org/10.1016/j.foodhyd.2022.107457.

[10] C. Pozo, S. Rodríguez-Llamazares, R. Bouza, et al., Study of the structural order of native starch granules using combined FTIR and XRD analysis, J. Polym. Res. 25 (2018) 266. https://doi.org/10.1007/s10965-018-1651-y.

[11] A. Hu, X. Chen, W. Wang, et al., Properties and structure of modified taro starch: comparison of ultrasound and malic acid treatments, Starch 73(9/10) (2021) 2000252. https://doi.org/10.1002/star.202000252.

[12] R.L. Hughes, W.H. Horn, P. Finnegan, et al., Resistant starch type 2 from wheat reduces postprandial glycemic response with concurrent alterations in gut microbiota composition, Nutrients 13(2) (2021) 645. https://doi.org/10.3390/nu13020645.

[13] N.J.W. Albrechtsen, J.F. Rehfeld, On premises and principles for measurement of gastrointestinal peptide hormones, Peptides 141(2021) 170545. https://doi:10.1016/j.peptides.2021.170545.

[14] X.G. Ji, K.L. Chang, M. Chen, et al., *In vitro* fermentation of chitooligosaccharides and their effects on human fecal microbial community structure and metabolites, LWT-Food Sci. Technol. 144 (2021) 111224. https://doi.org/10.1016/j.lwt.2021.111224.

[15] A.P.M. Kerckhoffs, M. Samsom, M.E. van der Rest, et al., Lower *Bifidobacteria* counts in both duodenal mucosa-associated and fecal microbiota in irritable bowel syndrome patients, World J. Gastroenterol. 15(23) (2009) 2887-2892. https://doi.org/10.3748/wjg.15.2887.

[16] J. Chen, Q. Chen, C. Xie, et al., Effects of simulated gastric and intestinal digestion on chitooligosaccharides in two *in vitro* models, Int. J. Food Sci. Tech. 55 (2019) 1881-1890. https://doi:10.1111/ijfs.14337.

[17] Q. Ye, F. Ge, Y. Wang, et al., Digestion of curcumin-fortified yogurt in short/long gastric residence times using a near-real dynamic *in vitro* human stomach, Food Chem. 372 (2022) 131327. https://doi.org/10.1016/j.foodchem.2021.131327.

[18] Y. Granfeldt, I. Björck, A. Drews, et al., An *in vitro* procedure based on chewing to predict metabolic response to starch in cereal and legume products, Eur. J. Clin. Nutr. 46(9) (1992) 649-660. https://doi:10.1093/ajcn/59.3.777S.

[19] A.J. Vela, M. Villanueva, Á.G. Solaesa, et al., Impact of high-intensity ultrasound waves on structural, functional, thermal and rheological properties of rice flour and its biopolymers structural features, Food Hydrocoll. 113 (2021) 106480. https://doi.org/10.1016/j.foodhyd.2020.106480.

[20] T. Hong, Y. Zhang, D. Xu, et al., Effect of sodium alginate on the quality of highland barley fortified wheat noodles, LWT-Food Sci. Technol. 140 (2021) 110719. https://doi.org/10.1016/j.lwt.2020.110719.

[21] S. Wang, S. Wang, L. Liu, et al., Structural orders of wheat starch do not determine the *in vitro* enzymatic digestibility, J. Agric. Food Chem. 65 (2017) 1697-1706. https://doi.org/10.1021/acs.jafc.6b04044.

[22] Y. Gu, X. Qian, B. Sun, et al., Nutritional composition and physicochemical properties of oat flour sieving fractions with different particle size, LWT-Food Sci. Technol. 154 (2022) 112757. https://doi.org/10.1016/j.lwt.2022.112757.

[23] G. Toffolo, F. De Grandi, C. Cobelli, Estimation of β-cell sensitivity from intravenous glucose tolerance test c-peptide data: knowledge of the kinetics avoids errors in modeling the secretion, diabetes, Diabetes 44(7) (1995) 845-854. https://doi.org/10.2337/diab.44.7.845.

[24] M.L. Johnson, T.W. Martens, A.B. Criego, et al., Utilizing the ambulatory glucose profile to standardize and implement continuous glucose monitoring in clinical practice, Diabetes Technol. Ther. 21(S2) (2019) S217-S225. https://doi:10.1089/dia.2019.0034.

[25] T.J. Little, S. Doran, J.H. Meyer, et al., The release of GLP-1 and ghrelin, but not GIP and CCK, by glucose is dependent upon the length of small intestine exposed, J. Appl. Physiol. Endocrinol. Metab. 291(3) (2006) e647-e655. https://doi:10.1152/ajpendo.00099.2006.

[26] D.I. Brierley, G. de Lartigue, Reappraising the role of the vagus nerve in GLP-1-mediated regulation of eating, Br. J. Pharmacol. 179 (2021) 584-599. https://doi:10.1111/bph.15603.

[27] A. Everard, C. Belzer, L. Geurts, et al., Cross-talk between *Akkermansia muciniphila* and intestinal epithelium controls diet-induced obesity, PNAS. 110(22) (2013) 9066-9071. https://doi:10.1073/pnas.1219451110.

[28] S.S. Al-Jameel, Association of diabetes and microbiota: an update, Saudi J. Biol. Sci. 28(8) (2021) 4446-4454. https://doi.org/10.1016/j.sjbs.2021.04.041.

[29] L. Bordalo Tonucci, K.M.O. Dos Santos, C.L. De Luces Fortes Ferreira, et al., Gut microbiota and probiotics: focus on diabetes mellitus, Crit. Rev. Food Sci. Nutr. 57(11) (2015) 2296-2309. https://doi.org/10.1080/10408398.2014.934438.

[30] J.Y. Wu, K. Wang, X.M. Wang, et al., The role of the gut microbiome and its metabolites in metabolic diseases, Protein Cell. 12(5) (2021) 360-373. https://doi.org/10.1007/s13238-020-00814-7.

[31] T.J. Wang, D. Ngo, N. Psychogios, et al., 2-Aminoadipic acid is a biomarker for diabetes risk, J. Clin. Invest. 123(10) (2013) 4309-4317. https://doi.org/10.1172/jci64801.

[32] W.Y. Xu, Y. Shen, H. Zhu, et al., 2-Aminoadipic acid protects against obesity and diabetes, J. Endocrinol. 243(2) (2019) 111-123. https://doi.org/10.1530/joe-19-0157.

[33] E.S. Yu, H.J. Min, K. Lee, et al., Anti-inflammatory activity of p-coumaryl alcohol-*γ*-*O*-methyl ether is mediated through modulation of interferon-*γ* production in Th cells, Br. J. Pharmacol. 156(7) (2009) 1107-1114. https://doi.org/10.1111/j.1476-5381.2009.00114.

[34] W.K. Chan, S.S. Tsai, Y.R. Li, et al., Association between serum bilirubin levels and progression of albuminuria in Taiwanese with type 2 diabetes mellitus, Biomed. J. 44(2) (2021) 201-208. https://doi.org/10.1016/j.bj.2019.12.004.

[35] A. Wahlström, I. Sayin Sama, H.U. Marschall, et al., Intestinal crosstalk between bile acids and microbiota and its impact on host metabolism, Cell Metab. 24(1) (2016) 41-50. https://doi.org/10.1016/j.cmet.2016.05.005.

[36] J. Lu, S. Wang, M. Li, et al., Association of serum bile acids profile and pathway dysregulation with the risk of developing diabetes among normoglycemic Chinese adults: findings from the 4C study, Diabetes Care 44(2) (2021) 499-510. https://doi.org/10.2337/dc20-0884.

[37] P.T. Clayton, E. Patel, A.M. Lawson, et al., Bile acid profiles in peroxisomal 3-oxoacyl-coenzyme A thiolase deficiency, J. Clin. Invest. 85(4) (1990) 1267-1273. https://doi.org/10.1172/jci114563.

[38] T. Furuya, M. Miura, M. Kuroiwa, et al., High-yield production of vanillin from ferulic acid by a coenzyme-independent decarboxylase/oxygenase two-stage process, N. Biotechnol. 32(3) (2015) 335-339. https://doi.org/10.1016/j.nbt.2015.03.002.

[39] Q.H. Chen, D.T. Xie, S. Qiang, et al., Developing efficient vanillin biosynthesis system by regulating feruloyl-CoA synthetase and enoyl-CoA hydratase enzymes, Appl. Microbiol. Biotechnol. 106(1) (2022) 247-259. https://doi.org/10.1007/s00253-021-11709-w.

[40] D. Grapov, S.H. Adams, T.L. Pedersen, et al., Type 2 diabetes associated changes in the plasma non-esterified fatty acids, oxylipins and endocannabinoids, PLoS One 7(11) (2012) e48852. https://doi.org/10.1371/journal.pone.0048852.

[41] G. Roda, S. Chien Ng, P.G. Kotze, et al., Crohn's disease, Nat. Rev. Dis. Primers 6(1) (2020) 22. https://doi.org/10.1038/s41572-020-0156-2.

[42] L. Hinshaw, M. Schiavon, A. Mallad, et al., Effects of delayed gastric emptying on postprandial glucose kinetics, insulin sensitivity, and β-cell function, Am. J. Physiol. Endocrinol. Metab. 307(6) (2014) E494-E502. https://doi.org/10.1152/ajpendo.00199.2014.

[43] D.D. Ramdath, Q. Liu, E. Donner, et al., Investigating the relationship between lentil carbohydrate fractions and *in vivo* postprandial blood glucose response by use of the natural variation in starch fractions among 20 lentil varieties, Food Funct. 8(10) (2017) 3783-3791. https://doi.org/10.1039/c7fo00972k.